*EVS26*
*Los Angeles, California, May 6-9, 2012*

# Pattern Recognition-Based State-of-Health Prediction for a PEM Fuel Cell

Jonghoon Kim[1], Changyoon Chun[1], Inhae Lee[2], Yongsug Tak[2], B. H. Cho[1]
[1]*School of Electrical Engineering and Computer Science, Seoul National University*
[2]*Department of Chemical Engineering, Inha University*

## Abstract

This work investigates a pattern recognition-based diagnosis approach as an application of the Hamming neural network to the identification of suitable fuel cell model parameters, which aim to diagnose state-of-health (SOH) for a polymer electrolyte membrane (PEM) fuel cell. The fuel cell output voltage (FCOV) patterns of the 20 PEM fuel cells were measured, together with the model parameters, as representative patterns. Through statistical analysis of the FCOV patterns for 20 single cells, the Hamming neural network is applied for identification of the representative FCOV pattern that matches most closely of the pattern of the arbitrary cell to be measured. Considering, the selected cell's $\Delta R_d$ is properly applied to diagnose SOH of an arbitrary cell through the comparison with those of fully fresh and aged cells with the minimum and maximum of the $\Delta R_d$ in experimental cell group, respectively.

*Keywords: Polymer electrolyte membrane fuel cell, Hamming network, state-of-health, Pattern recognition*

## 1 Introduction

The polymer electrolyte membrane (PEM) fuel cell are considered to be the most promising energy technology with the advantages of low-operating temperature, high current density, high potential for low cost and volume, fast start-up ability become the most promising and attractive candidate for electric vehicle power [1]. But, fuel cells still suffer from a low reliability and a short lifetime, which make them difficult to satisfy user's requirements. Moreover, when dealing with reliability and durability, the fuel cell diagnosis has been identified among the critical issues that need to be developed to increase system performance. The development of diagnostic can help evaluating the fuel cell state-of-health (SOH) [2][3]. Precise SOH diagnosis is critical in practical applications where it is necessary to determine how long the fuel cell will last, and to minimize the risk of permanent internal damage.

In general, fuel cell voltage is highly dependent to the pulse current. The magnitude of the decrease in this voltage, called the voltage variance, is associated with changes in fuel cell model parameters that include open circuit voltage (OCV; $E_{Nernst}$), three types of losses such as ohmic losses ($R_{ohm}$), activation losses ($R_{act}$) concentration losses ($R_{conc}$), and double layer capacitance ($C_{dl}$) [4][5]. Since these parameters vary with electrochemical characteristics, temperature and aging effect, the voltage variance can be used to determine the magnitude of the parameters for the fuel cell model. Specifically, two losses, namely, the activation losses and the concentration losses, are considered as critical factors that determine the magnitude of the voltage variance.

When a constant current is commonly applied to the cells, the magnitudes of the respective voltage variance are different. In addition, the fuel cell

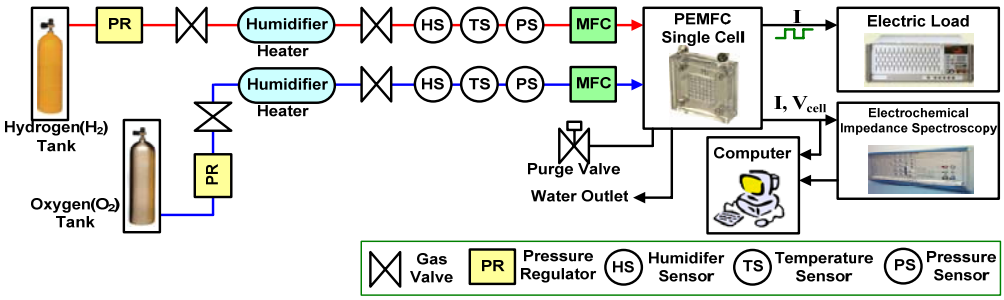


Figure1: Experimental setup for measuring the fuel cell output voltage (FCOV) pattern for 20 PEM fuel cells

output voltage (FCOV) pattern of each cell is almost constant under identical condition such as pulse current magnitude and time interval. Thus, the FCOV pattern can be used to discriminate among PEM fuel cells with different characteristics for improved SOH diagnosis. This investigation proposes the use of a Hamming neural network [6]-[8] for FCOV pattern recognition. The Hamming neural network is generally used and designed explicitly for binary pattern recognition. In this work, the Hamming neural network is used to evaluate several predetermined representative FCOV pattern and determine the one that is closest to the input FCOV pattern by comparing the inner product. Through the statistical analysis, the proposed method can perform recognition of an arbitrary FCOV pattern. Representative FCOV patterns are collected from 20 single cells, together with four characteristic parameters for each cell. Considering the equivalent circuit fuel cell model, a representative loss $\Delta R_d(R_{act}+R_{conc})$ defined as the sum of two losses (activation and concentration losses) of the selected representative FCOV pattern is properly applied to diagnose SOH of an arbitrary cell through the comparison with those of fully fresh and aged cells with the minimum and maximum of the $\Delta R_d$ in experimental cell group. Finally, these results enable us to provide interesting perspectives for diagnostic fuel cell SOH without the need for repeated parameter measurement.

## 2 Experimental setup

The experimental setup was designed for obtaining the representative FCOVs of the 20 PEM fuel cells by the 'Materials and Electro-Chemistry Laboratory in Inha University'. A block diagram of the setup is presented in Fig. 1. All experiments were conducted using a subscale single cell (active area of 25cm$^2$). The membrane electrode assembly that used was a GORE™ PRIMEA® SERIES 57 MEA (W. L. Gore & Associates, Inc.) that has 0.4mg/cm$^2$ Pt on both

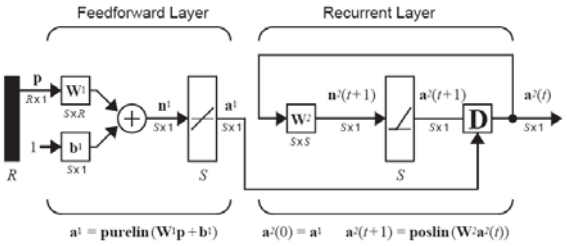


Figure2: Hamming neural network

the anode and the cathode. The GDLs were SIGRACET® GDL 10BB (thickness of 420 μm, SGL Carbon Japan Ltd.). High purity $H_2$ (99.99%) gas for the anode feed, high purity Air ($O_2$ 21%/ $N_2$) for the cathode feed, and high purity $N_2$ (99.99%) gas for both the anode and cathode feed were used. It is necessary to determine the maximum hydrogen/oxygen excess ratios to avoid hydrogen/oxygen starvation. The experiments were performed with $H_2$ and $O_2$ under the constant stoichiometry mode of $\lambda_{H_2}$=1and $\lambda_{O_2}$=1.5. The gas flow rates corresponding to a stoichiometry of 1 and 1.5 for $H_2$ and air are 150ml/min and 488ml/min with a constant pressure (101.325kPa), respectively. These gases were humidified in a bubbling humidifier before entering the fuel cell. The temperature of the cell was 70ºC and the humidification temperature was 70ºC (100% RH).

## 3 Hamming neural network

The Hamming neural network [6]-[8] is used for pattern recognition, as shown in Fig. 2. It is one of the simplest examples of a competitive network and is designed explicitly to solve binary pattern recognition issues. The Hamming network decides which representative pattern is closest to the current pattern by comparing the inner products.

### 3.1 Feedforward layer

The feedforward layer calculates a correlation or inner product between each representative pattern and the current pattern in order to find the Hamming distance (HD) from calculation the

difference between dimension $m$ and HD. In order to calculate the inner products, weight matrix $\mathbf{W^1}$ is a set of prototype vectors and is transformed into the binary form, in addition to bias vector, $\mathbf{b^1}$, in (1) and (2), respectively.

$$\mathbf{W}^1 = \begin{bmatrix} {}_1\mathbf{w}^{iT} \\ {}_2\mathbf{w}^{iT} \\ \vdots \\ {}_S\mathbf{w}^{iT} \end{bmatrix} = \frac{1}{2}\begin{bmatrix} {}_1\mathbf{w}^1 & {}_2\mathbf{w}^1 & \cdots & {}_S\mathbf{w}^1 \\ {}_1\mathbf{w}^2 & {}_2\mathbf{w}^2 & \cdots & {}_S\mathbf{w}^2 \\ \vdots & \vdots & \ddots & \vdots \\ {}_1\mathbf{w}^R & {}_2\mathbf{w}^R & \cdots & {}_S\mathbf{w}^R \end{bmatrix} = \begin{bmatrix} \mathbf{p}_1^T \\ \mathbf{p}_2^T \\ \vdots \\ \mathbf{p}_S^T \end{bmatrix} \quad (1)$$

$$\mathbf{b}^1 = [R, R, \cdots, R]^T = \left[\frac{m}{2}, \frac{m}{2}, \cdots, \frac{m}{2}\right]^T \quad (2)$$

where each row of $\mathbf{W^1}$ represents a prototype vector which it is required to be recognize, and each element of $\mathbf{b^1}$, $m/2$ is the threshold value and is set equal to the number of elements in each input vector $R$, $S$ is the number of neurons. As expressed in (3), it is high desirable to have the $i^{\text{th}}$ node ($1 \le i \le R$) node in this layer compute $m - \mathrm{HD}({}_i\mathbf{w}, \mathbf{p})$ for a given input vector $\mathbf{p}$, where $\mathrm{HD}({}_i\mathbf{w}, \mathbf{p})$ is the HD distance between vectors ${}_i\mathbf{w}$ and $\mathbf{p}$. Then, the net input of node is as in (4), namely, the feedforward layer output. Finally, these outputs are equal to the inner (Eq. (5)). The neuron in this layer with the largest output corresponds to the prototype pattern that is closest in HD to the input pattern.

$$\mathbf{W}^1\mathbf{p} = \left[m - \mathrm{HD}({}_i\mathbf{w}, \mathbf{p})\right] - \mathrm{HD}({}_i\mathbf{w}, \mathbf{p}) \quad (3)$$

$$\mathrm{net}_i = \mathbf{n}^1 = \mathbf{W}^1\mathbf{p} + \frac{m}{2} = m - \mathrm{HD}({}_i\mathbf{w}, \mathbf{p}) \quad i = 1, 2, \cdots, S \quad (4)$$

$$\mathbf{a}^1 = \mathbf{W}^1\mathbf{p} + \mathbf{b}^1 = \begin{bmatrix} \mathbf{p}_1^T\mathbf{p} + R \\ \mathbf{p}_2^T\mathbf{p} + R \\ \vdots \\ \mathbf{p}_S^T\mathbf{p} + R \end{bmatrix} = \mathbf{purelin}(\mathbf{W}^1\mathbf{p} + \mathbf{b}^1) \quad (5)$$

### 3.2 Recurrent layer

The recurrent layer is known as the MAXNET. It is a competitive layer that performs the winner-take-all (WTA) operation, whose purpose is to enhance the initial dominant response of the $i^{\text{th}}$ node and suppress the others [9]. The neurons are initialized with the outputs of the feedforward layer, which indicates the correlation between the prototype vectors and the input vector. As a result of recurrent processing, the $i^{\text{th}}$ node responds positively whereas the responses of all remaining nodes decay to zero. Thus, in order to determine a winner, as expressed in (6), the recurrent layer output is updated according to the following recurrence relation using a positive transfer function (**poslin**).

$$\mathbf{a}^2(t+1) = \mathbf{poslin}(\mathbf{W}^2\mathbf{a}^2(t)) \quad (6)$$

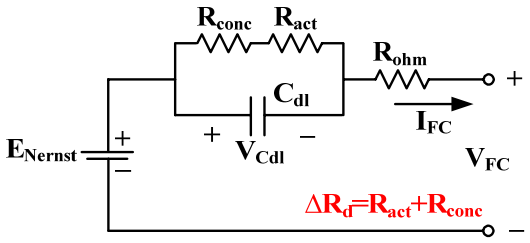


Figure3: Fuel cell equivalent circuit model

This processing requires self-feedback connections and negative lateral inhibition connections in which the output of each neuron has an inhibitory effect on all of the other neurons [9]. The $n \times n$ weight matrix of the recurrent layer $\mathbf{W^2}$ is taken in (7). The weights in this layer are set so that the diagonal elements are 1, and the off-diagonal elements have a small negative value, where $0 < \varepsilon < 1/(S-1)$ is called the lateral interaction coefficient. Thus, weight values of 1 and $-\varepsilon$ can be set for the appropriate elements of $\mathbf{W^2}$ in (8), where $1 \le i \le S$ and $1 \le j \le S$.

$$\mathbf{W}^2 = \begin{bmatrix} {}_1\mathbf{w}^1 & {}_1\mathbf{w}^2 & \cdots & {}_1\mathbf{w}^S \\ {}_2\mathbf{w}^1 & {}_2\mathbf{w}^2 & \cdots & {}_2\mathbf{w}^S \\ \vdots & \vdots & \ddots & \vdots \\ {}_i\mathbf{w}^1 & {}_i\mathbf{w}^2 & \cdots & {}_i\mathbf{w}^S \end{bmatrix} = \begin{bmatrix} 1 & -\varepsilon & \cdots & -\varepsilon \\ -\varepsilon & 1 & \cdots & -\varepsilon \\ \vdots & \vdots & \ddots & \vdots \\ -\varepsilon & -\varepsilon & \cdots & 1 \end{bmatrix} \quad (7)$$

$$\mathbf{a}_i^2(t+1) = poslin\left(\mathbf{a}_i^2(t) - \varepsilon\sum_{j \ne i}\mathbf{a}_j^2(t)\right) \quad (8)$$

Each neuron's output decreases in proportion to the sum of the other neuron's outputs. The output of the neuron with the largest initial output decreases more slowly than the outputs of the other neurons. But eventually, only one neuron will have a positive output. The index of the recurrent layer neuron with a stable positive output is the index of the prototype vector that is the best match with the input.

## 4 Proposed approach

The equivalent circuit for the charge double layer effect on the cell voltage is shown in Fig. 3. In this figure, $C_{dl}$ is the equivalent capacitance depending on the charge double layer. Since the electrodes of a PEM fuel cell are porous, the capacitance $C_{dl}$ is very large and can be in the order of several Farads [10]. $R_{ohm}$, $R_{act}$, and $R_{conc}$ are equivalent resistances to the ohmic, activation, and concentration overvoltages, respectively. $V_{Cdl}$ is the overvoltage due to the common effects of the double capacitive layer, the activation, and the concentration resistances. The double layer capacitive layer overvoltage follows the first-order dynamic (Eq. (9))

$$V_{Cdl} = \left(I_{FC} - C_{dl}\frac{dV_{Cdl}}{dt}\right)(R_{act} + R_{conc}) \quad (9)$$

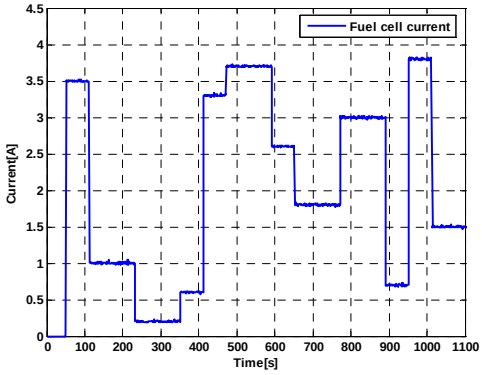


Figure4: Pulse current profile covering from 0~3.8A for obtaining the FCOV pattern

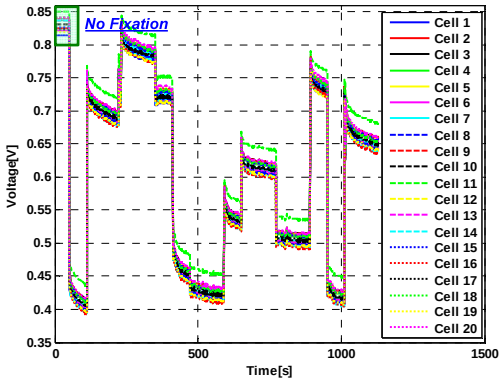


Figure5: Unfixed fuel cell output voltage (FCOV) patterns for 20 single cells

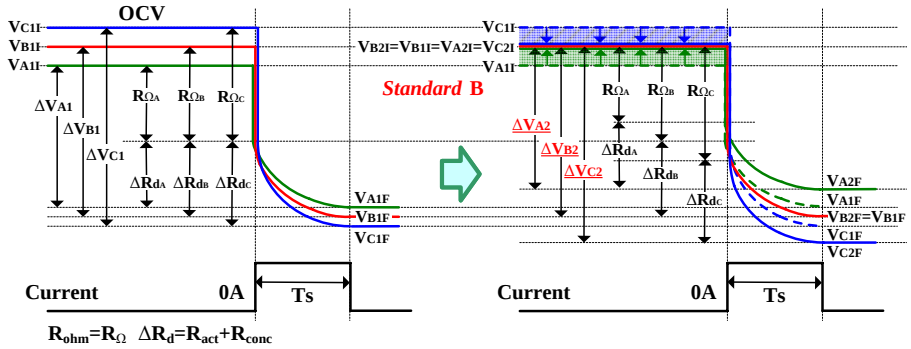


Figure6: A method to recognize the FCOV pattern through statistical analysis (ISVP fixation)

The transient performance of the fuel cell equivalent circuit model over short or long time period is differently observed [4]. In this work, however, it can be assumed that the fuel cell current has a step or a similar shape for a short or long time. In such cases, the $V_{Cdl}$ is calculated as in equation (9), and the voltage approximates to equation (10) after some time passes unless the current level changes significantly. Then, the sum of two resistances $R_{act}$ and $R_{conc}$ is defined as the magnitude of the $\Delta R_d$ in (11).

$$V_{Cdl} \approx I_{FC} \cdot (R_{act} + R_{conc}) \quad (10)$$

$$\Delta R_d = R_{act} + R_{conc} \quad (11)$$

The $\Delta R_d$ among the PEM fuel cells is frequently varied with electrochemical characteristics, temperature, and aging effect. As a result, the $\Delta R_d$ can be considered as an important factor to determine the PEM fuel cell SOH.

## 4.1 Fuel cell output voltage (FCOV)

The pulse current profile covering from 0A to 3.8A is applied to the fuel cell about 1100s, as shown in Fig. 4. Then, for a pulse current profile, the FCOV data collected is shown in Fig. 5. The FCOV pattern is recognized through experiments for 20 PEM fuel cells. For recognition of the FCOV pattern with the Hamming neural network, statistical analysis is absolutely necessary. Then, the initial starting points of each FCOV pattern should be fixed. However, as shown in Fig. 5, the initial starting voltage points (ISVP) of the 20 PEM fuel cells were not fixed due to their different electrochemical characteristics. Hence, the average and standard deviation of the 20 collected output voltages cannot be compared. Therefore, it is required to set a standard ISVP, as shown in Fig. 6. For example, consider three cells A–C with different ISVPs ($V_{A1I}$–$V_{C1I}$). If the standard fuel cell is set as B ($V_{B1I}$=$V_{B2I}$), then the voltages of A and C are higher and lower, respectively ($V_{A1I}$⇨$V_{A2I}$, $V_{C1I}$⇨$V_{C2I}$). Therefore, the three ISVPs are fixed at one point, as shown in Fig. 7. Based on this rule, the average and standard deviation of voltage A can be expressed in (12) and (13), respectively. The average (AVE) and standard deviation (STD) of three cells can be compared in (14) and (15).

$$\text{Fuel cell(A)}_{AVE} = \frac{\sum_{i=1}^{n} V_{A2i}}{n} \quad (n = 1, 2, \cdots, F) \quad (12)$$

$$\text{Fuel cell(A)}_{STD} = \sqrt{\frac{\sum_{i=1}^{n} \left(V_{A2i} - \text{Fuel cell(A)}_{AVE}\right)^2}{n}} \quad (13)$$

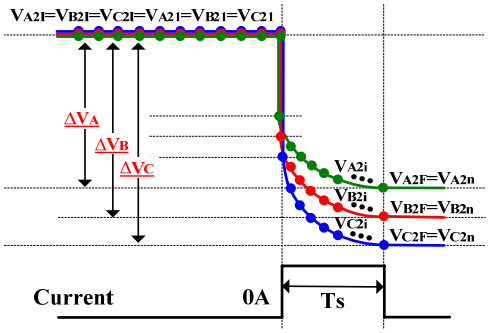


Figure7: Each FCOV pattern comparison after ISVP

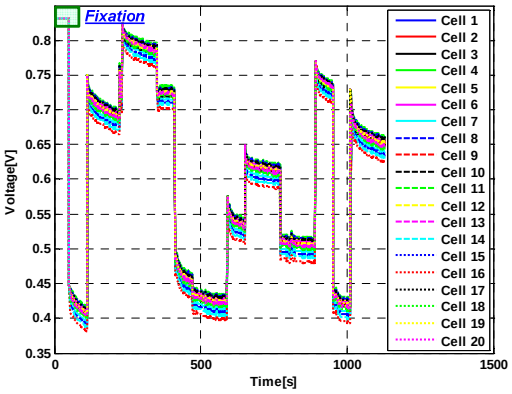


Figure8: Fixed FCOV patterns for 20 single cells

$$\text{Fuel cell(A)}_{AVE} > \text{Fuel cell(B)}_{AVE} > \text{Fuel cell(C)}_{AVE} \quad (14)$$

$$\text{Fuel cell(A)}_{STD} < \text{Fuel cell(B)}_{STD} < \text{Fuel cell(C)}_{STD} \quad (15)$$

The fixed FCOV patterns are given in Fig. 8. These results enable us to obtain the fixed ISVP (0.831V) among 20 PEM fuel cells. All averages and standard deviations for the collected FCOV patterns can be compared.

## 4.2 Characteristic parameters of the FCOV pattern

Table1: Four characteristic parameters for learning by the Hamming neural network

| | | |
|---|---|---|
| SVP | C1 | Standard deviations of the FCOV |
| AVP(f) | C2 | Average of the FCOV (f) |
| SVP(f) | C3 | Standard deviation of the FCOV (f) |
| MVP(f) | C4 | Minimum of the FCOV (f) |
| Standard : Cell No. 10; (f): fixation (ISVP) | | |

As indicated in Table 1, characteristic parameters C1-C4 are learned by the Hamming network using the average, standard deviation, and minimum of the FCOV patterns. Each value of the four characteristic parameters corresponding to the 20 representative FCOV patterns is transformed into 1 and -1 element array with four levels, as shown in Fig. 9. If these patterns are not transformed into this binary form of same norm, the pattern recognition performance can be distorted by the one parameter of C1-C4, which has the large real value. In Fig. 9, *avg* is the average and *std* is the standard deviation of each characteristic parameter. The levels of each parameter are decided by three standard, viz., *avg*-($\alpha \times std$), *avg*, and *avg*+($\alpha \times std$). The levels are decided according to the values of the parameter as shown in Fig. 10. For example, if the value is larger than *avg*-($\alpha \times std$) and smaller than *avg*, the level is L3. $\alpha$ is a tuning value and chosen 0.5 to make the characteristic differences.

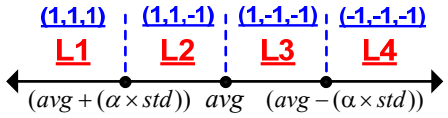


Figure9: Four levels as to three standards

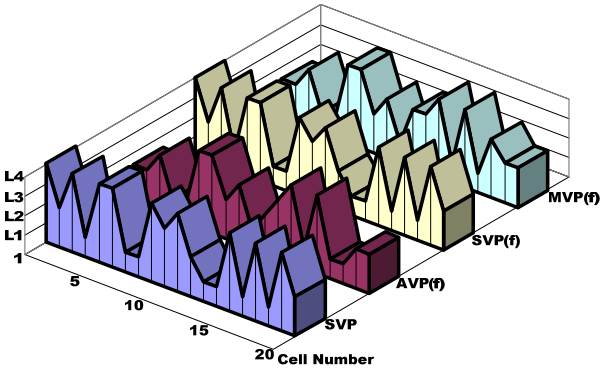


Figure10: Characteristics of four representative patterns

## 4.3 Pattern recognition with the Hamming neural network

As shown in Fig. 11, the feedforward layer calculates the inner product between each representative pattern and the current pattern. The value of each of the four characteristic parameters corresponding to 20 representative patterns is transformed into the binary form and stored in the weight matrix $\mathbf{W}^1$ as expressed in (16) and (17).

$$\mathbf{W}^1 = \begin{bmatrix} {}_1\mathbf{w}^{iT} \\ {}_2\mathbf{w}^{iT} \\ \vdots \\ {}_{20}\mathbf{w}^{iT} \end{bmatrix} = \frac{1}{2}\begin{bmatrix} {}_1w^1 & {}_2w^1 & \cdots & {}_{20}w^1 \\ {}_1w^2 & {}_2w^2 & \cdots & {}_{20}w^2 \\ \vdots & \vdots & \ddots & \vdots \\ {}_1w^{12} & {}_2w^{12} & \cdots & {}_{20}w^{12} \end{bmatrix} = \begin{bmatrix} \mathbf{p}_1^T \\ \mathbf{p}_2^T \\ \vdots \\ \mathbf{p}_{20}^T \end{bmatrix} \quad (16)$$

$$\mathbf{b}^1 = [12, 12, \cdots, 12] \quad (17)$$

The 20 neurons storing the results of the inner product in the feedforward layer compete with each other to determine a winner. Then, self-feedback connection and negative lateral inhibition connection are required to implement the WTA. As expressed in (18), the weights in the recurrent

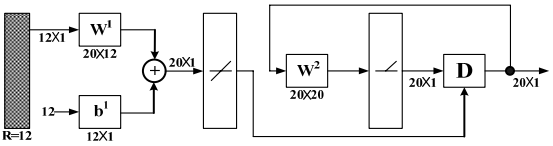


Figure11: Hamming neural network in this work

layer $\mathbf{W}^2$ are set so that the diagonal elements are 1, and the off-diagonal elements have a small negative value, where $0<\varepsilon<1/(20-1)$ is called the lateral interaction coefficient ($\varepsilon=0.01$). After the competition in (19), only one neuron will have a nonzero output, and this neuron indicates the representative pattern that is closest to a current pattern.

$$\mathbf{W}^2 = \begin{bmatrix} {}_1\mathbf{w}^1 & {}_1\mathbf{w}^2 & \cdots & {}_1\mathbf{w}^{20} \\ {}_2\mathbf{w}^1 & {}_2\mathbf{w}^2 & \cdots & {}_2\mathbf{w}^{20} \\ \vdots & \vdots & \ddots & \vdots \\ {}_i\mathbf{w}^1 & {}_i\mathbf{w}^2 & \cdots & {}_i\mathbf{w}^{20} \end{bmatrix} = \begin{bmatrix} 1 & -0.01 & \cdots & -0.01 \\ -0.01 & 1 & \cdots & -0.01 \\ \vdots & \vdots & \ddots & \vdots \\ -0.01 & -0.01 & \cdots & 1 \end{bmatrix} \quad (18)$$

$$\mathbf{a}_i^2(t+1) = \mathbf{poslin}\left(\mathbf{a}_i^2(t) - 0.01\sum_{j\neq i}\mathbf{a}_j^2(t)\right) \quad (19)$$

## 4.4 Verification

Table2: Representative loss $\Delta R_d$ results for 20 single cells after 25 seconds

| Cell | $\Delta R_d[\Omega]$ | Cell | $\Delta R_d[\Omega]$ | Cell | $\Delta R_d[\Omega]$ | Cell | $\Delta R_d[\Omega]$ |
|---|---|---|---|---|---|---|---|
| No.1 | 0.0052 | No.6 | 0.0062 | No.11 | 0.0044 | No.16 | 0.0133 |
| No.2 | 0.0070 | No.7 | 0.0097 | No.12 | 0.0078 | No.17 | 0.0056 |
| No.3 | 0.0073 | No.8 | 0.0108 | No.13 | 0.0080 | No.18 | 0.0087 |
| No.4 | 0.0083 | No.9 | 0.0072 | No.14 | 0.0117 | No.19 | 0.0066 |
| No.5 | 0.0058 | No.10 | 0.0076 | No.15 | 0.0049 | No.20 | 0.0074 |

Representative loss $\Delta R_d$ results for 20 single cells were previously measured after 25 seconds with the pulse current, and compared with those of arbitrary cells, as listed in Table 2. When the pulse current profile shown in Fig. 4 is applied to two arbitrary cells, the outputs of the two layers of the Hamming neural network for two arbitrary cells are shown in Fig. 12. In each case, we see that in the current layer, only the selected representative FCOV pattern has a non-zero output. As shown in Fig. 12(a), a representative loss $\Delta R_d$ of an arbitrary cell 1 (0.0106Ω) is similar with to that of the selected representative FCOV pattern (No.8; 0.0108Ω). In addition, the FCOV pattern of the No.17 (0.0056Ω) is selected as the representative FCOV pattern that is closest to the current FCOV pattern of an arbitrary cell 2 (0.0055Ω), as shown in Fig. 12(b).

## 4.5 SOH diagnosis

The representative loss $\Delta R_d$ of the selected FCOV pattern in Section 4.4 is properly applied

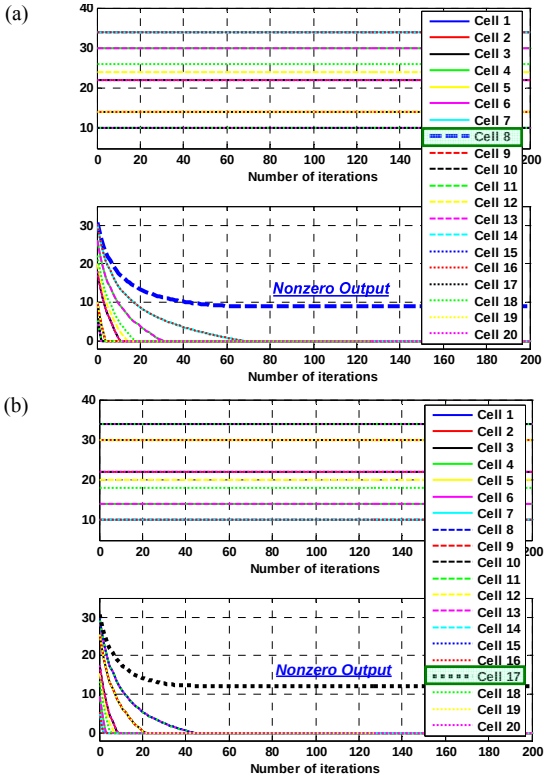


Figure12: Outputs of two layers by the Hamming neural network. (a) Arbitrary cell 1, selected fuel cell output voltage (FCOV) pattern : No. 8, (b) Arbitrary cell 2, selected FCOV pattern : No. 17

to diagnose SOH of an arbitrary cell through the comparison with those of fully fresh and aged cells with the minimum and maximum of the $\Delta R_d$ in experimental cell group, respectively. In (20), the SOH of an arbitrary cell can be diagnosed using the selected cell pattern's $\Delta R_d$, $\Delta R_d^{selected}$.

$$\underset{arbitrary}{SOH} = \left|\frac{\Delta R_d^{selected} - \Delta R_d^{aged}}{\Delta R_d^{fresh} - \Delta R_d^{aged}}\right| \quad (20)$$

where, $\Delta R_d^{fresh}$ (No.11; 0.0044Ω) and $\Delta R_d^{aged}$ (No.16; 0.0133Ω) are each $\Delta R_d$ values of fully fresh and aged cells among 20 single cells. The fully fresh cell has the largest SOH (SOH=1), on the other hand, the fully aged cell has the smallest SOH (SOH=0). 20 experimental single cells have each $\Delta R_d$ within this range of 0.0044–0.0133Ω. With obtained $\Delta R_d$ values (0.0108Ω and 0.0056Ω) of two arbitrary cells, the diagnosed SOHs of two arbitrary cells are expressed in (21) and (22), respectively. (SOH range: 0–1)

$$\underset{arbitrary1}{SOH} = \left|\frac{\Delta R_d^{selected} - \Delta R_d^{aged}}{\Delta R_d^{fresh} - \Delta R_d^{aged}}\right| = \left|\frac{0.0108 - 0.0133}{0.0044 - 0.0133}\right| \approx 0.2809 \quad (21)$$

$$\underset{arbitrary2}{SOH} = \left|\frac{\Delta R_d^{selected} - \Delta R_d^{aged}}{\Delta R_d^{fresh} - \Delta R_d^{aged}}\right| = \left|\frac{0.0056 - 0.0133}{0.0044 - 0.0133}\right| \approx 0.8651 \quad (22)$$

We can see, the range of SOH is from 0 to 1, and 1 means the cell is totally health, or it is new, and 0 means the cell cannot meet the power demand of the practical applications. These results enable to us to provide interesting perspectives for diagnostic fuel cell SOH without the need for repeated parameter measurement of an arbitrary cell. For reference, it is assumed that $R_{ohm}$ is constant (0.0955Ω) due to little difference in electrochemical characteristics compared with that of the $\Delta R_d$ among the cells.

# 5 Conclusion

Precise SOH diagnosis is critical in practical applications where it is necessary to determine how long the fuel cell will last, and to minimize the risk of permanent internal damage. Therefore, a method to diagnose SOH for a PEM fuel cell, using a pattern recognition based approach as an application of the Hamming neural network to the identification of suitable fuel cell model parameters, has been presented in this work. Through statistical analysis of the FCOV patterns for 20 single cells, the Hamming neural network is applied for identification of the representative FCOV pattern that matches most closely of the pattern of the arbitrary cell to be measured. The selected cell's $\Delta R_d$ is properly applied to diagnose SOH of an arbitrary cell through the comparison with those of fully fresh and aged cells with the minimum and maximum of $\Delta R_d$ in experimental cell group, respectively. This avoids the need for repeated parameter measurement of an arbitrary cell. Therefore, these results could lead to interesting perspectives for diagnostic fuel cell SOH.

# Acknowledgments

This work was supported by the New and Renewable Energy Program of the Korea Institute of Energy Technology Evaluation and Planning (KETET) grant funded by the Korea government Ministry of Knowledge Economy (No. 20104010100490).

# References

[1] P. Corbo, et. Al., *PEFC stacks as power sources for hybrid propulsion systems*, International Journal of Hydrogen Energy, 34(2009), 4635-4644

[2] T. Kurz, et. Al., *An impedance-based predictive control strategy for the state-of-health of PEM fuel cell stacks*, Journal of Power Sources, 180(2008), 742-747

[3] R. Onanena, et. Al., *Estimation of fuel cell operating time for predictive maintenance strategies*, International Journal of Hydrogen Energy, 35(2010), 8022-8029

[4] S. V. Puranik, et. Al., *State-space modelling of proton exchange membrane fuel cell*, IEEE Transactions on Energy Conversion, 25(2010), 804-813

[5] K. P. Adzakpa, et. Al., *PEM fuel cells modelling and analysis through current and voltage transient behaviors*, IEEE Transactions on Energy Conversion, 23(2008), 581-591

[6] K. Koutroumbas, et. Al., *Generalized Hamming networks and applications*, Neural Networks, 23(2005), 896-913

[7] L. Chen, et. Al., *Capacity analysis for a two-level decoupled Hamming networks for associative memory under a noisy environment*, Neural Networks, 20(2007), 598-609

[8] I. Meilijon, et. Al., *A single-iteration threshold Hamming network*, IEEE Transactions on Neural Network, 6(1995), 261-266

[9] M. T. Hagan, *Neural network design,* ISBN 0-9717321-0-8, Boston MA, PWS Publishing Co, 1995

[10] M. T. Iqbal, et. Al., *Simulation of a small wind fuel cell hybrid energy system*, Renewable Energy, 28(2003), 511-522

# Authors

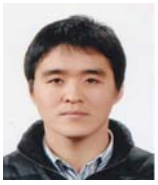

**Jonghoon Kim** received the B.S. degree in electrical engineering from Chungnam National University (CNU), Daejeon, Republic of Korea, in 2005, and received the Ph.D degree at Seoul National University (SNU), Seoul, Republic of Korea, in 2012. His main research interests include battery management system (BMS; modeling, screening, equalization, and SOC/SOH estimation), and fuel cell system (ripple current analysis, SOH prediction).

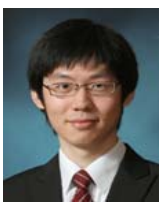

**Changyoon Chun** received his B.S. and M.S. degrees in 2009 and 2011, respectively, from Seoul National University (SNU), Seoul, Republic of Korea, where he is currently working toward the Ph.D. degree in the School of Electrical Engineering and Computer Science. His research interests are in the areas of resonant converters and battery management system.

**Inhae Lee** received the B.S. and M.S. degrees in electrical engineering from Inha University, Incheon, Republic of Korea, in 2010 and 2012, respectively. Her main research interests include Nano Materials & PEMFC.

**Yongsug Tak** received his B.S. and M.S. in Chemical Engineering from Seoul National University (SNU), Seoul, Republic of Korea, in 1984 and 1986, respectively. He received his Ph.D. in Chemical Engineering from Iowa State University in 1993. Prior to his research at Iowa State University, he worked as a Senior Researcher (Aug. 1993 – Feb. 1994) at Samsung Electro- Mechanics Co., Republic of Korea. Since 1994, he has been a Professor in Department of Chemical Engineering at Inha University. His current research interests include the etching and anodization of aluminum, polymer electrolyte membrane fuel cells (electrode materials and deactivation during long-term operation), and the electrochemical nanofabrication of functional materials.

**B. H. Cho** received the B.S. and M.S. degrees from California Institute of Technology, Pasadena, and the Ph.D. degree from Virginia Polytechnic Institute and State University (Virginia Tech), Blacksburg, all in electrical Engineering. Prior to his research at Virginia Tech, he worked as a member of Technical Staff with the Power Conversion Electronics Department, TRW Defense and Space System Group. From 1982 to 1995, he was a Professor with the Department of Electrical Engineering, Virginia Tech. In 1995, he joined School of Electrical Engineering, Seoul National University (SNU), Seoul, Republic of Korea, where he is currently a Professor. His current research interests include power electronics, modeling, analysis, and control of spacecraft power processing equipment, and distributed power systems. Dr. Cho was a recipient of the 1989 Presidential Young Investigator Award from the National Science Foundation. He chaired the 2006 IEEE Power Electronics Specialists Conference (PESC 2006). He is a member of Tau Beta Pi.